Zentrum für Technomathematik

Fachbereich 3 – Mathematik und Informatik

Tikhonov regularization for Electrical Impedance Tomography on unbounded domains

Michael Lukaschewitsch **Peter Maaß**
Michael Pidcock

Report 02–08

Berichte aus der Technomathematik

Report 02–08 **Oktober 2002**

Tikhonov regularization for Electrical Impedance Tomography on unbounded domains

Michael Lukaschewitsch[1], Peter Maass[2], Michael Pidcock[3]

[1] Lufthansa Systems Berlin GmbH, Fritschestr. 27–28, D-10585 Berlin
[2] Centre for Industrial Mathematics, University Bremen, D-28359 Bremen
[3] Department of Mathematical Sciences, Oxford Brookes University, Oxford OX33 1HX

Abstract

The mathematical analysis of geoelectric applications leads to the inverse problem of Electric Impedance Tomography (EIT) on unbounded domains. We introduce appropriate function spaces for this setting and discuss the analytic properties of the related forward operator on unbounded domains with Lipschitz boundaries. For the numerical approximation we consider Tikhonov regularization for a finite number of measurements. The main theorem states that this yields an approximation process which converges with an optimal rate to a minimum norm solution. Finally, numerical results in two and three dimensions, which are obtained from simulated, noisy data, confirm the theoretical findings.

Key words: Electrical impedance tomography, nonlinear inverse problems, Tikhonov regularization, geoelectric measurements

AMS subject classification: 65J22, 65R32

Acknowledgement: This work was partially supported by BMBF grant 03MSM1HB.

1 Introduction

A major application of geophysical imaging methods is in the exploration of the earth's interior. Data collected by making boundary, exterior or pointwise interior measurements are used to construct an image of the spatial variation of a parameter characterising structural variations within the earth's interior.

There are several methods currently in use, each based on the observation of a different physical effect. Examples include geomagnetic, seismic and geoelectric methods. Exterior measurements are used in gravimetric or magnetic approaches, whereas in ground water filtration, boundary measurements are used together with pointwise interior measurements, see, for example, [22] and literature cited there. Each of these methods depends on a special measurement process based on a specific physical model and the main task consists of an interpretation of the measured data using an inversion procedure.

The different approaches are complementary in that they cover a range of depths and resolutions as well as reconstructing different physical properties within the interior. For example, seismic methods are applied for recovering mass densities at depths from 10 m up to 6 km, whereas in geoelectric approaches the depth of investigation ranges from 10 cm to 100 m.

The geoelectric measurement process considered in this paper consists of using electrodes (metal stakes knocked into the earth) to inject electric current into the ground and measure the corresponding electrical potential at the surface, see Figure 1. The measured data depends on the spatial distribution of electrical conductivity (the parameter). The process which maps the parameter to the measured data (called the forward mapping or the forward operator) depends nonlinearly on the conductivity distribution and, consequently, the inverse problem of determining the parameter from the measured data is also nonlinear.

Figure 1: Multielectrode equipment

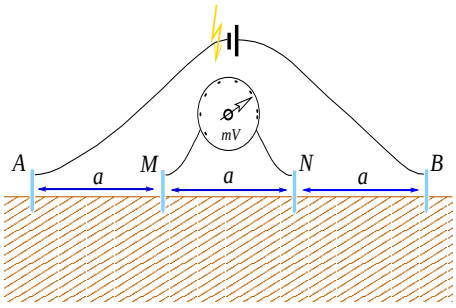

Figure 2: Wenner design

The inverse problem posed by geolectric applications is closely related to medical applications of Electrical Impedance Tomography (EIT). The mathematical descriptions of the geoelectric and medical applications of EIT are the same and the main difference is in the spatial extension of the domains being considered. In medical applications, the domain is bounded and the measurements cover all the accessible parts of the boundary. In geophysics the domain may be assumed to be unbounded, although the measurements on the boundary

are restricted to a finite part. Nevertheless, most results for the well-studied medical application carry over to unbounded domains relevant for geoelectric applications.

Regularity conditions on solutions of the elliptic partial differential equations that are used to model the physical situation imply that material discontinuities within the interior produce smooth boundary data and the effects of high frequency components of the conductivity are severely damped. Hence, the geoelectric inverse problem is also ill-posed and can only be solved approximately by using a suitable regularization method [18, 30]. This paper aims at analyzing Tikhonov regularization methods for geoelectric EIT.

1.1 Applications of geoelectric inversion

Geoelectrical imaging methods were originally used for geophysical and geological investigations but more recently the importance of these methods in environmental problems and archaeological investigations has been recognized.

The goal of geophysical and geological applications is the exploration of geological structures in the upper earth's crust at typical depths ranging from 10 m to 4000 m. Geoelectric inversion is frequently evaluated together with other methods and geological a-priori knowledge. Some examples of geophysical and geological applications are:

- Resistivity imaging of active volcanos: Changes in the chemical composition of volcanic gases and thermal changes deep in the interior also correlate to electric resistivity. Some recent work can be found in [21].

- Optimising geological drilling projects: geoelectric methods can be used to gain spatial information useful in determining optimal drilling locations. (cf. e.g. [39], [43]).

- Archaeological investigations: Here the main objective is to recover archaeological underground monuments, walls, cavities and settlements and the depth of investigation ranges from 1 m to 10 m e.g. obtaining plans of underground objects, investigations of structures inside buildings and monuments or the detection of man-made cavities such as cellars and underground corridors.

- Hydrogeological exploration and environmental investigations: This field is concerned with depths from 1 m to 50 m and has become one of the most important applications of geoelectric methods during the last 15 years. This field of applications includes investigation of infiltration processes, detection of ground water resources, evaluation of environmental impacts on ground water, exploration of former industrial and military sites, risk assessment of potential hazardous waste disposal sites, exploration of building sites, monitoring of (biochemical) remediation processes and mapping of water flow in the vicinity of dams and reservoirs.

1.1.1 Measurement techniques

Within the geoelectric community a number of different measurement schemes, i.e. electrode configurations, are considered: Wenner, Dipole - Dipole, Pole - Dipole and Pole - Pole. The frequently used Wenner design is illustrated in Figure 2: Electrodes which inject currents (A and B) and electrodes measuring surface potential differences (M and N) are laid out along a straight line separated by a constant distance a . When a measurement is completed, the entire configuration is moved by a distance a in one direction and the next measurement is taken. This is repeated several times starting from the same initial position using different values of a .

The classical geoelectric application does not utilize any mathematical inversion procedure. The data produced with one of these methods is only mapped to a subsurface profile taking into account the median depth of investigation covered by a single measurement. This mapping is called pseudosection or apparent resistivity and is used to represent measured data.

1.1.2 Standard inversion methods for geoelectric applications

Several mathematically motivated inversion procedures have been proposed for geoelectric applications.

The finite difference algorithm of Dey and Morrison[11] is used by many authors for the numerical solution of the forward problem in three space dimensions. This algorithm assumes that the conductivity distribution is constant in one direction (i.e. it is essentially two dimensional) and calculates potential distributions in the lower half-space.

A frequently applied inversion algorithm developed by Loke and Barker[29] uses a regularized Gauss-Newton method. In order to reduce computational costs, they also derived a quasi-Newton method where in each iteration the Jacobian matrix is updated by a rank one matrix (i.e. a Broyden update). The Jacobian is calculated only in the first iteration, assuming a constant background conductivity and using precomputed partial derivatives.

Ellis and Oldenburg [17] presented a nonlinear minimization approach, where a suitable objective function is minimized under the additional constraint that the residuum assumes a prescribed value depending on the data error. The objective function includes a priori knowledge and restricts the non uniqueness of the inverse problem.

Li and Oldenburg used an approximate inverse mapping ([28]).Using the Born approximation, one dimensional inversion is performed on Fourier transformed data. An inverse Fourier transformation then provides the approximate inverse. In each iteration step the model is updated by applying the approximate inverse to observed and predicted data. This recovers three dimensional conductivities but is restricted to the pole-pole layout.

1.2 Electrical Impedance Tomography (EIT)

The starting point of this paper is the well-developed theory for medical applications of EIT which we aim to transfer to unbounded domains as needed

for geoelectric applications. As well as the different support of the quantities involved medical applications have the advantage that measurements can be made on all accessible parts of the boundary; in geophysics the measurements on the boundary are restricted to a finite part. Our main convergence result for Tikhonov regularization, however, also applies to medical applications with objects of bounded support.

1.2.1 The mathematical model

Let $\Omega \subset \mathbb{R}^n (n = 2, 3)$ and suppose that $\sigma : \Omega \to \mathbb{R}$ is a strictly positive isotropic scalar conductivity distribution. If we assume that there are no current sources inside Ω then the electric potential u satisfies the partial differential equation

$$\nabla \cdot (\sigma \nabla u) = 0 \quad in\ \Omega. \tag{1}$$

Injecting currents along the boundary is modelled by assuming a knowledge of the current density function $j = \sigma \frac{\partial u}{\partial \nu}$ on the boundary of the object $\partial\Omega$. Throughout the paper, ν denotes the outer normal. Solving the partial differential equation (1) with the boundary condition $\sigma \frac{\partial u}{\partial \nu} = j$ for a current density $j \in H^{-1/2}(\partial\Omega)$, leads to a consideration of the transfer impedance operator

$$\begin{aligned} A_\sigma : H^{-1/2}(\partial\Omega) &\to H^{1/2}(\partial\Omega) && (2) \\ j &\mapsto u|_{\partial\Omega}. && (3) \end{aligned}$$

A_σ is the so called Neumann to Dirichlet operator.

The data for the inverse problem considered in this paper consists of a partial knowledge of A_σ in the form of a set $\{(j_1, u_1), \cdots, (j_n, u_m)\}$. Here each j_k is a current density function on the boundary, i.e. it consists of the values of the electrical current injected through each electrode, and the u_k consists of the resulting potential on the boundary, i.e. in a fully discrete setting it is a list of the potentials measured on the electrodes. In our case the domain Ω is the lower half-plane space including topographical deformations on the boundary. In other words, we are considering the problem in an unbounded region.

The precise definition of the forward operator will be given in Section 3.

1.2.2 Numerical methods

The use of electrical measurements on the boundary of human bodies for medical imaging started at the end of the 1970s. The technique was pioneered in the 1980s by Barber and Brown [2] using a backprojection technique for solving the linearized inverse problem using data obtained by injecting currents and measuring voltage differences via adjacent pairs of electrodes. Since that time there has been much effort devoted to the development of more rigorous algorithms and here we note just a few of the many subsequent developments.

Isaacson [24] introduced the idea of multiple electrode drives using optimal current patterns. Paulson et al [36] extended this concept to include the idea of optimal voltage measurements and implemented it using a regularized least squares Newton-based reconstruction algorithm based a formulation of EIT as

a problem in nonlinear optimization . Similar implementations using a variety of regularization methods have been reported by many groups.

More recently, attention has turned to methods based on the explicit use of a priori knowledge e.g. [20, 3, 9] and this has lead to development of a variety of different reconstruction algorithms including some based on integral equation methods e.g. [16, 23, 10, 38] or on the linear sampling method e.g.[5, 6, 7].

1.2.3 Uniqueness results

The unique solvability of the full nonlinear inverse problem has been investigated by many authors. The problem usually studied is: Given the entire Neumann-to-Dirchlet mapping A_σ what are the regularity conditions for which the conductivity σ is uniquely determined by A_σ. Some papers work with an equivalent problem posed by the adjoint Dirchlet-to-Neumann map Λ_σ.

This problem was first considered by Calderón in a famous and elusive paper [8] in which he proved the unique solvability of the linearized inverse problem. The first uniqueness result on the nonlinear problem was obtained by Kohn and Vogelius [26, 27]. They proved that if $\partial\Omega$ is C^∞ then piecewise analytic conductivity coefficients σ are uniquely determined by the boundary data Λ_σ. Alessandrini [1] extended these results to Lipschitz domains. Isakov [15] considered the case of piecewise constant conductivities. Sylvester and Uhlmann [40] proved uniqueness for $n \geq 3$, $\sigma \in C^\infty(\overline{\Omega})$ and Ω with C^∞ boundary $\partial\Omega$. Their assumptions were gradually relaxed by various authors and the result holds even for $\sigma \in W^{2,\infty}(\Omega)$, [41, 32] as well as for Lipschitz domains [1]. Nachman [33] proved uniqueness for $n \geq 2$ for conductivities $\sigma \in W^{2,p}(\Omega)$, $p > n/2$ on Lipschitz domains. For $n = 2$ this result was improved by Brown and Uhlmann [4] for conductivities $\sigma \in W^{1,p}(\Omega)$, $p > 2$. Recently Druskin [13]obtained a result for $\Omega = R^3_-$, under the assumption that there exists a partitioning of Ω into a finite set of subdomains with piecewise smooth boundaries within each of which conductivity is constant.

1.3 Structure of this paper

In this paper we will consider a number of aspects of geoelectric EIT. In Section 2 we will introduce appropriate function spaces for dealing with the inverse problem of EIT on unbounded domains. In Section 3 we discuss properties of weak solutions on unbounded domains and it is shown that Neumann boundary value problems are uniquely solvable (in the weak sense) even on unbounded domains. We will define the forward operator, i.e. the parameter-to-solution mapping, by means of a coercive trilinear form and analyze its differentiability.

In Section 4 we outline the theory of nonlinear inverse problems used in this paper and 4 and discuss the well-known result by Engl, Kunisch and Neubauer [19] on convergence rates. This will lead to the main theoretical result of this paper, namely a convergence result for a Tikhonov inversion procedure for EIT, which is also valid in the medical context.

Finally, in Section 5 we give some examples of numerical results.

2 Function spaces and imbedding theorems

In this section we will introduce appropriate function spaces for dealing with EIT on unbounded domains Ω. Sobolev spaces are well studied if $\Omega = \mathbb{R}^n$ or $\Omega = \mathbb{R}^n_-$, the half space with $x_n \leq 0$, see e.g. [25, 42]. However, typical domains, which we will consider, should be suitable for applications in geophysics, i.e. such domains should allow topographical deformations on the boundary and we have to generalize the standard results accordingly.

An appropriate choice of weight function will lead to suitable inhomogeneous Sobolev spaces and corresponding

- compact imbedding theorems,
- trace theorems,
- Poincaré inequalities,

even for unbounded domains with Lipschitz boundaries.

As the primary aim of this section is to prepare the necessary notation for the subsequent main chapters of this article, most results are stated without proof. The proofs can be found in the related chapters in [31],which is also available via http://math.uni-bremen.de/zetem/~mluka .

2.1 Weighted function spaces on unbounded domains

When dealing with Neumann problems of the type

$$\nabla \cdot (\sigma \nabla u) = 0 \quad \text{in} \quad \Omega \tag{4}$$

$$\sigma \frac{\partial u}{\partial \nu} = j \quad \text{on} \quad \partial\Omega, \tag{5}$$

representing the physical process of injecting a current j into an unbounded domain Ω one cannot use the usual Sobolev space $W^1(\Omega)$ because, in general, solutions for these problems are not square integrable in Ω.

Example: *Let Ω be the half-space R^3_-, set $\sigma \equiv 1$ and $j(s) = (1 + \|s\|^2)^{-\frac{3}{2}}$ for $s \in \partial\Omega = \mathbb{R}^2 \times \{0\}$. Then a solution is given by $u(x) = \|(x_1, x_2, x_3 - 1)\|^{-1}$, which is not square integrable in $\mathbb{R}^3_-$.*

To consider functions for such problems, we follow the approach in [25], where weighted Sobolev spaces are introduced to solve elliptic boundary value problems on unbounded domains. Throughout this article, we use a simple type of weight $\rho(x) = (1 + |x|)^\alpha$, where $\alpha > 1$.

We now review some frequently used notations and introduce the basic concepts of weighted Sobolev spaces. At the beginning we allow general open domains $\Omega \subseteq \mathbb{R}^n$. This will later be restricted to domains with Lipschitz boundaries in order to obtain imbedding theorems and Poincaré inequalities.

Definition 2.1 *Let $\Omega \subseteq \mathbb{R}^n$ be an open set. We use the following notation:*

$$C^\infty(\Omega) := \{f : \Omega \to \mathbb{R} \mid f \text{ is differentiable infinitely often in } \Omega\},$$

$$C^\infty_a(\Omega) := \{f \in C^\infty(\Omega) \mid |f(x)| \to 0 \text{ as } |x| \to \infty\},$$

Definition 2.2 *Let $\rho : \mathbb{R}^n \to \mathbb{R}_+$, $\rho(x) = (1+|x|)^\alpha$, $\alpha > 1$, be a weight. On the spaces C_a^∞ and C^∞ the weighted scalar product*

$$\langle f, g \rangle_{1,\rho} := \int_\Omega \rho(x)^{-2} f(x) g(x)\, dx + \sum_{i=1}^{n} \int_\Omega \partial_i f(x) \partial_i g(x)\, dx, \tag{6}$$

induces the norm

$$\|f\|_{1,\rho} := \left(\langle f, f \rangle_{1,\rho}\right)^{1/2} = \left(\|\rho^{-1} f\|^2_{L^2(\Omega)} + \||\nabla f|\|^2_{L^2(\Omega)}\right)^{1/2}. \tag{7}$$

Note that only the function f is multiplied with the weight function ρ.

Now we give a definition of weighted Sobolev spaces (on possibly unbounded domains), which corresponds to the classical inhomogeneous Sobolev spaces.

Definition 2.3 *The norm (7) is used to define the Sobolev spaces*

$$H^{1,\rho}(\Omega) := \overline{\left\{ f \in C^\infty(\Omega) \mid \|f\|_{1,\rho} < \infty \right\}}^{\|\cdot\|_{1,\rho}}, \tag{8}$$

$$H_a^{1,\rho}(\Omega) := \overline{\left\{ f \in C_a^\infty(\Omega) \mid \|f\|_{1,\rho} < \infty \right\}}^{\|\cdot\|_{1,\rho}}, \tag{9}$$

i.e., $H^{1,\rho}(\Omega)$ and $H_a^{1,\rho}(\Omega)$ are completions of suitable C^∞- functions with respect to the norm $\|\cdot\|_{1,\rho}$.

2.2 Imbedding theorems

In order to obtain compact imbeddings of $H^{1,\rho}(\Omega)$ and $H_a^{1,\rho}(\Omega)$ into $L^2(\Omega)$ we restrict the domains Ω under consideration to open subsets of $\mathbb{R}^n$ with Lipschitz boundaries $\partial\Omega$. Moreover the construction of the necessary extension operators described below requires that the non-smooth part of the boundary is restricted to a compact set and that the number of smooth patches needed to cover $\partial\Omega$ is finite. Such domains are suitable for modelling EIT applications in geophysics. We define the notion of a geophysical domain:

Definition 2.4 *A domain $\Omega \subset \mathbb{R}^n$ for which there exists a compact subset $S \subset \mathbb{R}^n$ such that*

i) $\Omega \setminus S = \mathbb{R}^n_- \setminus S$ and

ii) Ω has a Lipschitz boundary

is called a geophysical domain.

An illustration of such a domain is given in Figure 3.

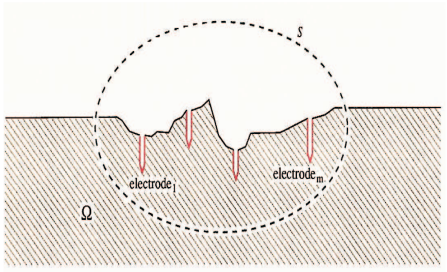

Figure 3: An illustration of a geophysical domain.

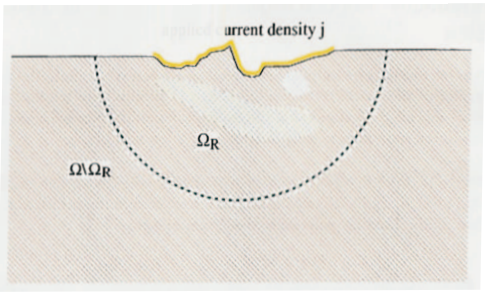

Figure 4: Partition of Ω.

For such domains we obtain linear and continuous extension operators by generalising the construction introduced in [25].

Lemma 2.5 *Let Ω be a geophysical domain and $\rho(x) = (1+|x|)^\alpha$, $\alpha > 1$, a weight. Then there exist linear and continuous extension operators $F : H^{1,\rho}(\Omega) \to H^{1,\rho}(\mathbb{R}^n)$ and $F_a : H_a^{1,\rho}(\Omega) \to H_a^{1,\rho}(\mathbb{R}^n)$, with $F(u)|_\Omega = u$ and $F_a(u)|_\Omega = u$.*

The existence of such extension operators is sufficient to obtain compact imbeddings for weighted Sobolev spaces on unbounded domains, see[25, 31]. We define a multiplication operator as follows.

Definition 2.6 *Let $\rho : \mathbb{R}^n \to \mathbb{R}_+$ be a weight. The mapping M_ρ is defined by the formula $M_\rho(f) := \rho^{-1} f$, for every measurable function $f : \Omega \to \mathbb{R}$.*

We now obtain the required compact imbeddings for suitable weight functions.

Theorem 2.7 *Let Ω be a geophysical domain and $\rho(x) = (1+|x|)^\alpha$ a weight.*
If $n \geq 2$ and $\alpha > n/2$ then $M_\rho : H^{1,\rho}(\Omega) \to L^2(\Omega)$ is a compact imbedding.
If $n = 3$ and $\alpha > 1$, then $M_\rho : H_a^{1,\rho}(\Omega) \to L^2(\Omega)$ is a compact imbedding.

2.3 Trace theorems and Poincaré inequalities

In subsequent sections the restriction of differentiable functions to the boundary $\partial\Omega$ will be used frequently. Hence, we will present a trace theorem for weighted Sobolev spaces from [25], which is natural when compared with standard results for unweighted Sobolev spaces on bounded domains and which we extend using compactness.

Theorem 2.8 *Let Ω be a geophysical domain, i.e. an unbounded domain with a locally finite Lipschitz boundary $\partial\Omega$. Further, let $\rho(x) = (1+|x|)^\alpha$ be a weight and $\alpha > 1$. Then there exists a linear and continuous map $\gamma : H^{1,\rho}(\Omega) \to L^{2,\rho}(\partial\Omega)$ such that $\gamma(u) = u|_{\partial\Omega}$ for all $u \in C^1(\overline{\Omega}) \cap H^{1,\rho}(\Omega)$.*
Additionally, if there exists an extension operator and if $n \geq 2$ and $\alpha > n/2$ then, the trace operator $\gamma : H^{1,\rho}(\Omega) \to L^{2,\rho}(\partial\Omega)$ is compact.
The same assertions are valid for $\gamma : H_a^{1,\rho}(\Omega) \to L^{2,\rho}(\partial\Omega)$, where $n = 3$ and $\alpha > 1$ is sufficient for the compactness of the trace operator γ.

We conclude this section by proving a Poincaré type inequality for such function spaces.

Definition 2.9 *Let $\mathcal{W}$ be a function space such that $1 \in \mathcal{W}$, where 1 denotes the function which assumes the constant value one. A continuous linear functional $\Gamma : \mathcal{W} \to \mathbb{R}$ is called normalizing if $\Gamma(1) \neq 0$, i.e., $1 \notin \mathrm{Ker}(\Gamma)$.*

Theorem 2.10 *Let Ω be an unbounded geophysical domain, $\rho(x) := (1+|x|)^\alpha$ a weight and Γ a continuous linear normalizing functional. Then the following conditions lead to Poincaré inequalities :*

i) If $n \geq 2$ and $\alpha > n/2$, then there exists a constant $C > 0$ such that for all $u \in H^{1,\rho}(\Omega)$

$$\|u\|^2_{1,\rho} \leq C \left(\int_\Omega |\nabla u(x)|^2 dx + \Gamma(u)^2 \right) \tag{10}$$

ii) If $n = 3$ and $\alpha > 1$ then there exists a constant $C > 0$ such that for all $u \in H^{1,\rho}_a(\Omega)$

$$\|u\|^2_{1,\rho} \leq C \left(\int_\Omega |\nabla u(x)|^2 dx \right) \quad . \tag{11}$$

Proof: i) Note that the assumption $\alpha > n/2$ implies $1 \in H^{1,\rho}(\Omega)$. Assuming that the assertion is false implies the existence of a sequence $\{u_n\}_{n\in\mathbb{N}}$ with $u_n \in H^{1,\rho}(\Omega)$ and $\|u_n\|_{1,\rho} = 1$ such that

$$\frac{1}{n} > \int_\Omega |\nabla u_n(x)|^2 dx + \Gamma(u_n)^2 \tag{12}$$

holds for all $n \in \mathbb{N}$.
This implies that $\lim_{n\to\infty} \||\nabla u_n|\|_{L^2(\Omega)} = 0$ and $\|u_n\|_{1,\rho} = 1$ for all $n \in \mathbb{N}$. Theorem 2.7 can be applied, to give a subsequence (denoted again by $\{u_n\}_{n\in\mathbb{N}}$) such that $M_\rho(u_n) = \rho^{-1}u_n$ is L^2-convergent to some element in $L^2(\Omega)$. Hence, the sequence $\{u_n\}_{n\in\mathbb{N}}$ is a Cauchy-sequence in $H^{1,\rho}(\Omega)$, and there exists an element $g \in H^{1,\rho}(\Omega)$ such that $\lim_{n\to\infty} \|u_n - g\|_{1,\rho} = 0$.
Since $\lim_{n\to\infty} \||\nabla u_n|\|_{L^2(\Omega)} = 0$ we have $\partial_i g = 0$ almost everywhere in Ω for each $i \in \{1, \cdots, n\}$. It follows that there exists a constant $c_0 \in \mathbb{R}$ such that $g(x) = c_0$ for almost every $x \in \Omega$. Equation (12) gives

$$\lim_{n\to\infty} \Gamma(u_n) = 0. \tag{13}$$

Since Γ is continuous and linear it follows that

$$\lim_{n\to\infty} \Gamma(u_n) = \Gamma(g) = c_0\Gamma(1). \tag{14}$$

This implies that $c_0 = 0$ and therefore

$$\lim_{n\to\infty} u_n = 0 \text{ in } H^{1,\rho}(\Omega). \tag{15}$$

This conclusion contradicts the assumption $\|u_n\|_{1,\rho} = 1$.

ii) By the assumption on the asymptotic behaviour $|x| \to \infty$ it follows that $1 \notin H_a^{1,\rho}(\Omega)$. An argument similar to that in i) provides a sequence $u_n \in H_a^{1,\rho}(\Omega)$ such that $\|u_n\|_{1,\rho} = 1$, $\lim_{n\to\infty} \|u_n - g\|_{1,\rho} = 0$ for a $g \in H_a^{1,\rho}(\Omega)$ and $g = c_0$ for some constant. Since $1 \notin H_a^{1,\rho}(\Omega)$ it follows that $g = 0$ and the same contradiction as in i) is established. $\diamond$

Examples of normalizing functionals: *For* $1 \in H^{1,\rho}(\Omega)$, *i.e.* $\alpha > n/2$ *consider the functionals*

$$\Gamma_1(u) := \int_{\partial\Omega} u(s)\rho(s)^{-2} d\mathcal{S} \quad \textit{and} \tag{16}$$

$$\Gamma_2(u) := \int_S u(s) d\mathcal{S}, \tag{17}$$

where $S \subset \partial\Omega$ *denotes a bounded subset as in the definition of geophysical domains.*
The trace theorem (Theorem 2.8) and the Cauchy-Schwarz inequality lead to the estimate

$$\begin{aligned} |\Gamma_1(u)|^2 &= \left| \int_{\partial\Omega} \frac{1}{\rho(s)} \frac{u(s)}{\rho(s)} d\mathcal{S} \right|^2 \\ &\leq \int_{\partial\Omega} \frac{1}{\rho(s)^2} d\mathcal{S} \int_{\partial\Omega} \frac{u(s)^2}{\rho(s)^2} d\mathcal{S} \leq c\|u\|_{1,\rho}^2, \end{aligned} \tag{18}$$

i.e., Γ_1 *is continuous. For* Γ_2 *the estimate*

$$\begin{aligned} |\Gamma_2(u)|^2 &\leq \max_{t\in S} \rho(t)^4 \left(\int_S \left| \frac{u(s)}{\rho(s)^2} \right| d\mathcal{S} \right)^2 \leq \\ &\leq c \int_S \frac{1}{\rho(s)^2} d\mathcal{S} \int_{\partial\Omega} \frac{u(s)^2}{\rho(s)^2} d\mathcal{S} \leq c'\|u\|_{1,\rho}^2 \end{aligned} \tag{19}$$

proves continuity. The normalizing property of these two functionals is clear.

3 Properties of the forward operator

For the formulation of the forward operator we assume that a known current density j is injected on the boundary $\partial\Omega$. The forward operator then maps the parameter σ to the solution of the Neumann boundary problem

$$\begin{aligned} \nabla \cdot (\sigma \nabla u) &= 0 \quad \text{in} \quad \Omega \,, \\ \sigma \frac{\partial u}{\partial \nu} &= j \quad \text{on} \quad \partial\Omega. \end{aligned}$$

For a complete model of geophysical EIT we will later combine this forward operator with the restriction of the solution u to its values on the boundary. For most of this chapter we investigate the properties of the forward operator for a single measurement, i.e. for injecting a single current density j. Motivated by applications in geophysics, we assume, that the support of j is compact.

The weak formulation for this Neumann boundary value problem and its properties are well known. However, we use a slightly different approach which is more suitable for treating the inverse problems in the subsequent sections. To achieve compatibility with the following sections the usual bilinear forms are substituted by trilinear forms, where the coefficient σ is introduced as an additional variable.

Definition 3.1 *Let $\mathcal{H} = H^{1,\rho}(\Omega)$ or $\mathcal{H} = H^{1,\rho}_a(\Omega)$ and $j \in L^2(\partial\Omega)$ with bounded support. Then the trilinear form $T : L^\infty(\Omega) \times \mathcal{H} \times \mathcal{H} \to \mathbb{R}$ and the linear form $L_j : \mathcal{H} \to \mathbb{R}$ are defined by*

$$T(\sigma, u, v) := \int_\Omega \sigma(x) \nabla u(x) \nabla v(x) dx, \tag{20}$$

$$L_j(v) := \int_{\partial\Omega} j(s) v(s) d\mathcal{S} \tag{21}$$

for all $\sigma \in L^\infty(\Omega)$.
Moreover, for a given $c_0 > 0$ let $Q \subset L^\infty(\Omega)$ denote a set of uniformly strictly positive parameters, i.e., the set of all functions σ such that $\sigma \geq c_0$ a.e. in Ω.

A function $u \in \mathcal{H}$ is called a weak solution of the Neumann boundary problem if

$$T(\sigma, u, v) = L_j(v) \;,\; \forall v \in \mathcal{H} \;. \tag{22}$$

In order to apply the Lax-Milgram Theorem for proving existence and uniqueness of a weak solution we have to analyze the coercivity of the trilinear form.

Proposition 3.2 *The linear forms from Definition 3.1 are continuous.*
For $\alpha > n/2$, $n \geq 2$ let

$$\mathcal{H} := \left\{ u \in H^{1,\rho}(\Omega) \mid \Gamma(u) = 0 \right\}, \tag{23}$$

where Γ denotes a normalizing functional (cf. Definition 2.9).
For $n = 3$ and $\alpha > 1$ let

$$\mathcal{H} = H^{1,\rho}_a(\Omega). \tag{24}$$

If $Q \subset L^\infty(\Omega)$ is a set of uniformly strictly positive parameters, then the trilinear form $T : L^\infty(\Omega) \times \mathcal{H} \times \mathcal{H} \to \mathbb{R}$ is uniformly coercive for all $\sigma \in Q$.

Proof: The continuity of $T : L^\infty(\Omega) \times \mathcal{H} \times \mathcal{H} \to \mathbb{R}$ is clear.
Note that for the linear form L_j the support of j was assumed to be compact. Then the estimate

$$\begin{aligned} |L_j(v)| &\leq \int_{\mathrm{supp}(j)} |j(s)||v(s)| d\mathcal{S} \\ &\leq \max_{s \in \mathrm{supp}(j)} \rho(s) \|j\|_{L^2(\partial\Omega)} \|\rho^{-1} v\|_{L^2(\partial\Omega)} \end{aligned} \tag{25}$$

together with Theorem 2.8 proves continuity for the linear form $L_j : \mathcal{H} \to \mathbb{R}$. Theorem 2.10 provides the estimate

$$\|u\|^2_{1,\rho} \leq C \int_\Omega |\nabla u(x)|^2 dx, \tag{26}$$

for all $u \in \mathcal{H}$ which leads directly to the uniform coercivity of T in Q, i.e.,

$$\begin{aligned} \|u\|^2_{1,\rho} &\leq C \int_\Omega |\nabla u(x)|^2 dx \\ &\leq C c_0^{-1} \int_\Omega \sigma(x) \nabla u(x) \nabla u(x) dx \\ &= C c_0^{-1} T(\sigma, u, u). \end{aligned} \tag{27}$$

$\diamond$

The Lax-Milgram Theorem now guarantees that for each $\sigma \in Q$ and each $j \in L^2(\partial\Omega)$ with bounded support there is a unique solution $u \in \mathcal{H}$ of the (weak) Neumann boundary value problem (22).

For a definition of the forward operator, which maps a parameter σ to the solution u, we formalise the use of the trilinear form T as follows.

Lemma 3.3 *Let $\mathcal{H}$ denote either $H^{1,\rho}(\Omega)$ or $H^{1,\rho}_a(\Omega)$ and let $Q \subset L^\infty(\mathbb{R}^n)$ denote a subset of uniformly strictly positive parameters with $\sigma > c_0 > 0$. Let T denote a trilinear form*

$$T : L^\infty(\mathbb{R}^n) \times \mathcal{H} \times \mathcal{H} \to \mathbb{R}$$

which is a uniformly coercive mapping for all $\sigma \in Q$. Let $\mathcal{H}^*$ denote the dual space of $\mathcal{H}$. Then the following statements hold.

1. *For each $\sigma \in L^\infty(\mathbb{R}^n)$, $u \in \mathcal{H}$ we have*

$$T(\sigma, u, \cdot) \in \mathcal{H}^* \text{ and } \|T(\sigma, u, \cdot)\|_{\mathcal{H}^*} \leq c_L \|\sigma\|_{L^\infty(\mathbb{R}^n)} \|u\|_{\mathcal{H}} \quad .$$

Therefore, the linear mapping

$$u \mapsto T(\sigma, u, \cdot) : \mathcal{H} \to \mathcal{H}^*$$

is continuous for each fixed $\sigma \in L^\infty(\mathbb{R}^n)$, i.e.,

$$T(\sigma, \cdot, \cdot) \in L(\mathcal{H}, \mathcal{H}^*) \text{ and } \|T(\sigma, \cdot, \cdot)\|_{L(\mathcal{H}, \mathcal{H}^*)} \leq c_L \|u\|_{L^\infty(\mathbb{R}^n)} \quad .$$

2. *For each $\sigma \in Q$ there exists a continuous mapping $T_\sigma^{-1} \in L(\mathcal{H}^*, \mathcal{H})$ with $\|T_\sigma^{-1}\| \leq \mathcal{C}$, which is the inverse of $T(\sigma, \cdot, \cdot)$, i.e.,*

   $T(\sigma, T_\sigma^{-1} g, \cdot) = g(\cdot)$ *for each* $g \in \mathcal{H}^*$ *and* $T_\sigma^{-1} T(\sigma, u, \cdot) = u$ *for each* $u \in \mathcal{H}$.

3. *In the following, the abbreviation T_σ is used instead of $T(\sigma, \cdot, \cdot)$. Then by the previous statement $T_\sigma T_\sigma^{-1} = Id_{\mathcal{H}^*}$ and $T_\sigma^{-1} T_\sigma = Id_{\mathcal{H}}$ holds for each $\sigma \in Q$.*

4. *The mappings $\sigma \mapsto T_\sigma : L^\infty(\mathbb{R}^n) \to L(\mathcal{H}, \mathcal{H}^*)$ and $\sigma \mapsto T_\sigma^{-1} : Q \to L(\mathcal{H}^*, \mathcal{H})$ are continuous.*

Proof:

1. This follows directly from the definition of T.

2. The existence of the inverse mapping $T_\sigma^{-1} \in L(\mathcal{H}^*, \mathcal{H})$ and the estimate $\|T_\sigma^{-1}\| \leq \mathcal{C}$ for each $\sigma \in Q$ follow directly from the Lax-Milgram Theorem for coercive linear forms.

3. This is a reformulation of the previous statement.

4. The estimate $\|T_\sigma\|_{L(\mathcal{H}, \mathcal{H}^*)} \leq c_L \|\sigma\|_{L^\infty(\mathbb{R}^n)}$ is obvious and provides continuity of the mapping $\sigma \mapsto T_\sigma : L^\infty(\mathbb{R}^n) \to L(\mathcal{H}, \mathcal{H}^*)$. For the continuity of $\sigma \mapsto T_\sigma^{-1}$ let $\sigma, \sigma' \in Q$ and consider

$$\begin{aligned} \|T_\sigma^{-1} - T_{\sigma'}^{-1}\| &= \|T_{\sigma'}^{-1} (T_{\sigma'} - T_\sigma) T_\sigma^{-1}\| \\ &\leq \|T_{\sigma'}^{-1}\| \|T_{\sigma'} - T_\sigma\| \|T_\sigma^{-1}\| \\ &\leq \mathcal{C}^2 c_L \|\sigma' - \sigma\|. \end{aligned} \tag{28}$$

◇

Remark: The operator T_σ introduced above depends linearly on the parameter σ, i.e. $T_{\sigma+\sigma'} = T_\sigma + T_{\sigma'}$. However, the inverse operator T_σ^{-1} is only defined on the subset Q, where it depends non-linearly on σ.

Hence, we obtain the solution of the Neumann boundary problem (22), by

$$u = T_\sigma^{-1} L_j \ .$$

We have to combine this with the trace operator

$$\gamma : H^{1,\rho}(\Omega) \to L^{2,\rho}(\partial\Omega)$$

in order to obtain the complete parameter-to-solution mapping, i.e. the forward operator for a single measurement with current density j:

Definition 3.4

$$A_{L_j} : Q \to L^2(\partial\Omega)$$
$$\sigma \mapsto \gamma(u) = \gamma \circ T_\sigma^{-1} L_j$$

denotes the parameter-to-solution map.

This definition extends easily to multiple measurements.

Definition 3.5 *Let $\{j_k\}_{k\in\{1,\cdots,m\}}$ be a set of compactly supported current densities in $L^2(\partial\Omega)$. Then the parameter-to-solution mappings of the previous definition are used to define the forward operator A by*

$$A \quad : \quad Q \to \prod_{k=1}^{m} L^{2,\rho}(\partial\Omega), \tag{29}$$

$$A_k \quad := \quad A_{L_{j_k}}, \tag{30}$$

where A_k denotes the k^{th} component of the operator A.

Finally we will analyze the differentiability of the forward operator with respect to the parameter σ for a single measurement. In order to abbreviate our notation we use $A := A_{L_j}$.

Theorem 3.6 *Let the assumptions of Lemma 3.3 be satisfied. For a fixed $\sigma \in Q$ choose $\varepsilon > 0$ sufficiently small such that the ball $\mathcal{B}_\varepsilon(\sigma) \subset Q$ and $\varepsilon < \frac{1}{\mathcal{C}c_L}$. Then the formula*

$$A(\sigma + h) = A(\sigma) + \gamma \circ \left(\sum_{\ell=1}^{\infty} \left(-T_\sigma^{-1} T_h \right)^\ell \right) \; (T_\sigma^{-1} L_j) \tag{31}$$

is valid for all $h \in \mathcal{B}_\varepsilon(0)$.

Proof: Since $A = \gamma \circ T_\sigma^{-1} L_j$ we have to analyze the non-linear dependence of T_σ^{-1} on σ. This is done by working as much as possible with T_σ, which depends linearly on σ.
For a fixed j denote $g := L_j \in \mathcal{H}^*$ and $\mathcal{A}(\sigma) := T_\sigma^{-1} g$.
For $h \in \mathcal{B}_\varepsilon(0)$ let us denote $\sigma' := \sigma + h$, $y_\sigma := \mathcal{A}(\sigma) = T_\sigma^{-1} g$, $y_{\sigma'} := \mathcal{A}(s') = T_{\sigma'}^{-1} g$ and $z := y_{\sigma'} - y_\sigma$.
By Lemma 3.3 we have $T_\sigma y_\sigma = g$ and $T_{\sigma'} y_{\sigma'} = g$ which leads to

$$\begin{aligned} T_\sigma y_\sigma &= T_{\sigma'}(y_\sigma + z) \\ &= T_{(\sigma+h)} y_\sigma + T_{(\sigma+h)} z \\ &= T_\sigma y_\sigma + T_h y_\sigma + T_\sigma z + T_h z. \end{aligned} \tag{32}$$

This is equivalent to

$$T_\sigma z + T_h z = -T_h y_\sigma. \tag{33}$$

As T_σ is invertible, z satisfies the equation

$$\left(Id_{\mathcal{H}} + T_\sigma^{-1} T_h \right) z = -T_\sigma^{-1} T_h y_\sigma \; . \tag{34}$$

z can be written in terms of a Neumann series representation

$$z = \mathcal{A}(\sigma + h) - \mathcal{A}(\sigma) = \left(\sum_{\ell=0}^{\infty} \left(-T_\sigma^{-1} T_h \right)^\ell \right) \left(-T_\sigma^{-1} T_h \right) y_\sigma \tag{35}$$

if $\|-T_\sigma^{-1}T_h\| < 1$. This is ensured by the assumption on ε since $\|-T_\sigma^{-1}T_h\| \leq \mathcal{C}c_L \underbrace{\|h\|}_{<\varepsilon}$.

The result follows by replacing $y_\sigma = \mathcal{A}(\sigma)$ and by combining the Neumann series with the linear and continuous trace operator γ. $\diamond$

The previous Theorems lead directly to an explicit description of derivatives of the parameter-to-solution mapping A.

Corollary 3.7 *Let the assumptions of Theorem 3.6 be satisfied. The first derivative of the forward operator A_{L_j} at σ is given by the linear operator*

$$D_1 : \mathcal{B}_\varepsilon(\sigma) \subset Q \subset L^\infty(\mathbb{R}^n) \to L^2(\partial\Omega)$$

$$h \mapsto D_1 h = -\gamma \circ T_\sigma^{-1} T_h T_\sigma^{-1} L_j \ .$$

Similarly, the higher order terms in the Neumann expansion lead to explicit representations of higher order derivatives of A.

Remark: *The mapping $A : Q \to Y$, for $Q \subset P$ open, is of class C^ℓ for every natural number ℓ, i.e., it is of class C^∞. The ℓ^{th} derivative of A at $\sigma \in Q$ is the ℓ-linear mapping which is obtained with the help of the symmetrizing operator S^ℓ, which sums over all permutations of $(h_1, .., h_\ell)$, as follows:*

$$\frac{\partial^\ell}{\partial\sigma^\ell} A(\sigma; h_1, .., h_\ell) = \gamma \circ \left(S^\ell \prod_{k=1}^{\ell} T_\sigma^{-1} T_{h_k} \right) T_\sigma^{-1} L_j \ .$$

4 Tikhonov regularization for geoelectric impedance tomography

In this section we present the main result of this paper: a proof of convergence for Tikhonov regularization applied to the inverse problem of electrical impedance tomography on unbounded domains Ω.

To be more precise, we will discuss the realistic situation, where a finite number of current densities, $j_k, k = 1, .., m$ are injected and the resulting potentials u_k are measured on $\partial\Omega$. From this partial knowledge of the Neumann-to-Dirichlet map of the boundary value problem

$$\begin{aligned} \nabla \cdot (\sigma \nabla u) &= 0 \quad \text{in} \quad \Omega \,, \\ \sigma \frac{\partial u}{\partial \nu} &= j \quad \text{on} \quad \partial\Omega \end{aligned}$$

we try to compute an approximation to the parameter σ. We consider approximations obtained by minimizing appropriate Tikhonov functionals.
Let us first consider, what can be done with just one measurement. The forward operator for a given current density j, which maps the parameter σ to u on $\partial\Omega$, is given by $A(\sigma) = \gamma \circ T_\sigma^{-1} L_j$. This operator has been analyzed in the previous section.
Let y^δ denote noisy, measured data, which is assumed to have a limited accuracy, i.e. $||y - y^\delta||$ and $y = A(\sigma)$. The norms are taken in $L^2(\partial\Omega)$. In accordance with the general theory for non-linear inverse problems, we assume, that an *a priori* model σ^* has been chosen. We then compute an approximation σ_α^δ by minimizing the Tikhonov functional

$$F(\sigma) = ||A(\sigma) - y^\delta||^2 + \alpha ||\sigma - \sigma^*||^2 \,.$$

4.1 Tikhonov regularization for non-linear inverse problems

The best we can hope for – in a nonlinear inverse problem – is to define a rule for choosing $\alpha = \alpha(\delta)$ in such a way, that σ_α^δ converges to a σ^*-minimum norm solution as $\delta \to 0$. For an introduction to regularization theory for non-linear operator equations and the concept of σ^*-minimum norm solutions, we refer the reader to [18].
The following fundamental result concerning the convergence of Tikhonov regularizers for non-linear inverse problems was proved in [19].

Theorem 4.1 *Let X, Y denote Hilbertspaces. Let $A : \mathcal{D}(A) \subset X \to Y$ be a continuous nonlinear operator between Hilbert spaces. Let $\delta > 0$ and $y^\delta \in Y$ be such that $\|y - y^\delta\|_Y < \delta$. Further, let the following assumptions on A hold :*

1. *$\mathcal{D}(A)$ is convex,*
2. *A is weakly sequentially closed,*
3. *a σ^*-minimum-norm solution s^+ exists,*
4. *A is (Fréchet-)differentiable in a ball $\mathcal{B}_\rho(\sigma^+)$,*

5. *the derivative* $A'(\sigma^+) \in L(X,Y)$ *is Lipschitz continuous, i.e.,* $\|A'(\sigma^+) - A'(\sigma)\|_{L(X,Y)} \leq L\|\sigma^+ - \sigma\|_X$, *for all* $\sigma \in \mathcal{B}_\rho(\sigma^+)$, *where* L *denotes the Lipschitz constant,*

6. *let there exist an element* $w \in Y$ *satisfying* $\|\sigma^+ - \sigma^* - A'\,(\sigma^+)^*\, w\|_X = 0$, *where* $L\|w\|_Y \leq c_0 < 1$, *for a* $c_0 > 0$.

Then, if $\rho > 2\|\sigma^+ - \sigma^*\|_X + \sqrt{\frac{\delta_0}{K}}$, *where* $\delta_0 > 0$ *is such that* $\delta < \delta_0$ *for all error levels* $\delta > 0$ *of consideration, for the parameter choice* $\alpha := K\delta$, *where* K *denotes some positive constant, the asymptotic estimates*

$$\|A(\sigma_\alpha^\delta) - y^\delta\|_Y \leq \left(1 + \frac{2Kc_0}{L}\right)\delta \qquad \text{and} \tag{36}$$

$$\|\sigma_\alpha^\delta - \sigma^+\|_X \leq \frac{1}{\sqrt{1-c_0}}\left(\frac{1}{\sqrt{K}} + \frac{\sqrt{K}c_0}{L}\right)\delta^{\frac{1}{2}} \tag{37}$$

are valid.

Remark: *Assumption 6 is concerned with the smoothness of the solution and can be relaxed in different ways. For example, a practical relaxation of this restriction can be achieved as follows: let* $\vartheta \in \mathbb{R}$ *be positive such that there exists an element* $w_\vartheta \in Y$ *satisfying* $\|\sigma^+ - \sigma^* - A'\,(\sigma^+)^*\, w_\vartheta\|_X < \vartheta$, *where* $L\|w_\vartheta\|_Y \leq c_0 < 1$, *for a* $c_0 > 0$. *The error estimates of the above Theorem have to be adapted accordingly:*

$$\|A(\sigma_\alpha^\delta) - y^\delta\|_Y \leq \left(1 + \frac{2Kc_0}{L}\right)\delta + \sqrt{2\rho K}\;\delta^{\frac{1}{2}}\;\vartheta^{\frac{1}{2}} \qquad \text{and} \tag{38}$$

$$\|\sigma_\alpha^\delta - \sigma^+\|_X \leq \frac{1}{\sqrt{1-c_0}}\left(\left(\frac{1}{\sqrt{K}} + \frac{\sqrt{K}c_0}{L}\right)\delta^{\frac{1}{2}} + \sqrt{2\rho}\;\vartheta^{\frac{1}{2}}\right) \tag{39}$$

The proof of this generalisation which circumvents rather restrictive a priori assumptions on σ^* *can be found in [31]and it will be published in a more accessible form in a forthcoming paper.*

4.2 The parameter-to-solution mapping for a single measurement

The assumptions which are needed in the previous theorem to ensure the convergence of Tikhonov regularization are entirely formulated in terms of the forward operator. The forward operator of EIT has been studied in the previous section but we need two more prerequisites in order to apply the convergence theorem to EIT:

1. The results of the previous section were formulated for parameters $\sigma \in L^\infty(\Omega)$, the convergence theorem requires Hilbert spaces.

2. The forward operator needs to be weakly sequentially closed.

Restricting the domain of the parameter-to-solution mapping to a suitable subset of $L^\infty(\Omega)$ together with a Sobolev imbedding theorem leads to a variant of the forward mapping to which a convergence analysis can be applied. To simplify the following steps, Sobolev spaces with fractional order will be avoided and the following well known variant of imbedding is used :

Theorem 4.2 *Let $\Omega \subset \mathbb{R}^n$ be a bounded domain with Lipschitz boundary. If $k > \frac{n}{2}$, then the imbedding*

$$i : H^k(\Omega) \hookrightarrow \mathcal{C}^0(\overline{\Omega}) \tag{40}$$

is continuous and compact. Further, let $\Omega' \subset \mathbb{R}^n$ be such that $\Omega \subset \Omega'$ and

$$i' : \mathcal{C}^0(\overline{\Omega}) \hookrightarrow L^\infty(\Omega') \tag{41}$$

the operator which extends each $f \in \mathcal{C}^0(\overline{\Omega})$ to $L^\infty(\Omega')$ by setting its values to zero on $\Omega' \setminus \Omega$. Then obviously, i' is injective and continuous.

In order to achieve compatibility with this imbedding theorem we have to discuss the structure of the parameter σ as it appears in geophysical applications. The domain of definition Ω was introduced in Chapter 2 as a subset of $\mathbb{R}^n$, which combines the lower half space with a compact subset $S \subset \mathbb{R}^n$ with a Lipschitz boundary, i.e. this model includes local topological features like rocks, hills or even the shape of the electrodes used in the measurement. This assumption is natural for our field of applications, where we seek a local analysis of the underground region and the measurements are restricted to a finite number of electrodes in a finite region of interest. We further assume, that the values of the parameter σ at locations which are far away from the measurement positions only weakly influence the measurements in an averaged way.

It is therefore acceptable to choose an arbitrarily large but fixed ball $B(0,R) \subset \mathbb{R}^n$ of radius R at the origin and to assume that a rough model $\sigma_0 > 0$ on $\Omega / B(0,R)$ is known and sufficient for our approximations, see Figure 4. For example σ_0 might be a constant function, which represents the average electric conductivity of the upper earth surface. Then a suitable subset of $H^2(\Omega \cap B_R(0))$ will be chosen as domain of the forward operator.

Definition 4.3 *Let Ω denote a geophysical domain. Define $\Omega_R = \Omega \cap B_R(0)$ and let $P \subset H^2(\Omega_R)$ be a uniformly strictly positive subset, i.e, there exists a constant $c_0 > 0$ such that $\sigma \geq c_0$ on Ω_R for all $\sigma \in P$.*
For each bounded and strictly positive $\sigma_0 \geq c_0 > 0$ let $P_{\sigma_0} := P - \sigma_0$ be the affine translation of P.

Definition 4.4 *Let the space dimension $n = 2$ or $n = 3$ and Ω be an unbounded geophysical domain. Further, let $P \subset H^2(\Omega_R)$ be given by definition 4.3 and consider the compact imbedding $i : H^2(\Omega_R) \hookrightarrow \mathcal{C}^0(\overline{\Omega_R})$. For a given $\sigma_0 \geq c_0 > 0$*

and a given compactly supported current density $j \in L^2(\partial\Omega)$, the imbedded parameter-to-solution mapping A_j is defined by,

$$A_j : \quad P_{\sigma_0} \subset H^2(\Omega_R) \to L^{2,\rho}(\partial\Omega) \tag{42}$$

$$A_j(\sigma) := \gamma \circ A_{L_j}(\sigma_0 + \cdot) \circ i' \circ i \quad . \tag{43}$$

Corollary 4.5 *Let $P \subset H^2(\Omega_R)$ be given by definition 4.3. Then, the parameter-to-solution mapping $A_j : P_{\sigma_0} \subset H^2(\Omega_R) \to L^{2,\rho}(\partial\Omega)$ defined by (43) is a continuous operator with a Lipschitz continuous first derivative on each open ball $B \subset P_{\sigma_0}$.*

Proof: The imbeddings $i : H^2(\Omega_R) \hookrightarrow \mathcal{C}^0(\overline{\Omega_R})$ and $i' : \mathcal{C}^0(\overline{\Omega_R}) \hookrightarrow L^\infty(\Omega)$ are linear and continuous, as well as the trace operator $\gamma : \mathcal{H} \to L^2(\partial\Omega)$. The affine mapping $\sigma \mapsto \sigma_0 + \sigma : L^\infty(\Omega) \to L^\infty(\Omega)$ is obviously C^∞. Note that for the previously defined $P_{\sigma_0} \subset \mathcal{C}^0(\overline{\Omega})$ there exists an open uniformly positive subset $Q \subset L^\infty(\Omega)$ such that $\sigma_0 + i'(P_{\sigma_0}) \subset Q$. By Theorem 3.7 and the subsequent remark A_{L_j} is C^∞ on Q. We therefore obtain the C^∞ property of the composition (43) on each open ball $B \subset P_{\sigma_0}$.

Remark: *As in the previous section we can extend this result and obtain that the forward operator is C^∞ on P_{σ_0}.*

Finally, we need to show, that the mapping A_j is weakly sequentially closed. Again, we exploit the compactness of the imbedding $i : H^2(\Omega_R) \hookrightarrow \mathcal{C}^0(\overline{\Omega_R})$ and a result from [12]:

Proposition 4.6 *Let X, Y, Z be Banach spaces, $\mathcal{D}(\mathcal{A}) \subset \mathcal{X}$ a weakly sequentially closed subset and let $A : \mathcal{D}(\mathcal{A}) \to \mathcal{Y}$ be a nonlinear operator, which can be decomposed into a compact linear operator $K : X \to Z$ and a continuous nonlinear mapping $f : K(\mathcal{D}(\mathcal{A})) \subset \mathcal{Z} \to \mathcal{Y}$, i.e., $A = f \circ K$. Then A is weakly sequentially closed.*

In our situation the compact linear operator is provided by the imbedding operator. We immediately obtain the following result.

Corollary 4.7 *The forward operator $A_j : P_{\sigma_0} \subset H^2(\Omega_R) \to L^{2,\rho}(\partial\Omega)$ is weakly sequentially closed, of class C^∞ on each open ball $B \subset P_{\sigma_0}$ and hence has a Lipschitz continuous first derivative there.*

4.3 Convergence of Tikhonov regularization

In the previous sections we have proved all necessary properties of the forward operator in order to apply the convergence theory for non-linear Tikhonov regularization. Before stating the final result we want to summarize all the conditions that were necessary to obtain these results:

1. the domain of definition Ω is a geophysical domain, see Definition 2.4,

2. the current densities $j_k \in L^2(\partial\Omega), k = 1, .., m$ are compactly supported,

3. the current densities j_k have to satisfy $\Gamma(j_k) = 0$, if the space of potentials is chosen to be $H^{1,\rho}(\Omega)$, see Theorem 3.2 ,

4. a bounded and strictly positive approximation σ_0 is supposed to be known on $\Omega/B(R,0)$, where $B(R,0)$ denotes an arbitrarily large but fixed ball,

5. the parameter-to-solution mapping is defined on A_{σ_0}, see Definition 4.4.

Note that the domain of definition for the parameter-to-solution consists of functions σ with bounded support. However, we still require the theory developed in the previous sections for parameters on Ω, since the EIT differential equation has to be solved for $\sigma_0 + \sigma$ which is defined on the full unbounded domain Ω.

We now define the operator for a finite number of injected current densities.

Definition 4.8 *Let $\{j_k\}_{k\in\{1,\cdots,m\}}$ be a set of compactly supported current densities in $L^2(\partial\Omega)$. Then the parameter-to-solution mappings 43 are used to define the forward operator A by*

$$A \quad : \quad P_{\sigma_0} \subset H^2(\Omega_R) \to \prod_{k=1}^{m} L^{2,\rho}(\partial\Omega), \tag{44}$$

$$A_k \quad := \quad \gamma \circ A_{h_{j_k}}(\sigma_0 + \cdot) \circ i' \circ i, \tag{45}$$

where A_k denotes the k^{th} component of the operator A.

The final result now states that Tikhonov regularization can be applied to reconstruct an approximation to σ from a finite number of EIT measurements. More precisely, with a finite number of measurements we cannot expect that the Tikhonov approximation yields the true σ^{++} even with perfect data. However, we can prove that the Tikhonov regularization with a finite number of measurements converges (as the data error $\delta \to 0$) to a parameter σ, which provides the same data as σ^{++} and minimizes the distance to σ^*.

Theorem 4.9 *Let $A(\sigma)$ be defined by Definitions 4.8 and 4.4. and suppose that the assumptions 1..5 hold. Then the minimizer σ_α^δ of*

$$||A(\sigma) - y^\delta||^2 + \alpha||\sigma^* - \sigma||^2$$

converges to a σ^* minimum norm solution and

$$||\sigma_\alpha^\delta - \sigma^*|| = O(\delta^{1/2}) \ .$$

Proof: Theorem 4.1 and Corollary 4.7.

5 Numerical Experiments

The theoretical discussion presented in the previous sections of this paper lead us to an implementation of nonlinear Tikhonov regularization where the main task is the minimization of the nonlinear Tikhonov functional, see Section 4. This is achieved by a Gauss-Newton minimization procedure which requires a repeated evaluation of the forward mapping, its derivative and the adjoint of its derivative. Since weak formulations exist for all these operators the finite element method was chosen as an efficient tool for the implementation.

5.1 Implementation of the forward problem

There has been much discussion in the medical EIT literature of the need to use accurate models of the electrodes used in the procedure and of the resulting singular behaviour of the derivatives of the potential near the edges of the electrodes. This is reflected by the need to refine the finite element meshes in these regions, see ([34]). To achieve accurate evaluation of the operators required for the nonlinear minimization, the adaptive finite element code "KASKADE 3.0" has been modified to solve various boundary value problems with respect to different electrode models. "KASKADE 3.0" was developed at the Konrad-Zuse-Zentrum in Berlin [35], [37]. A major advantage of this software is the use of nonuniform adaptive meshes to increase accuracy of solutions. The program automatically refines meshes with respect to an *a posteriori* error estimation where solutions of higher order are compared locally with the solution of lower order. This leads to a criterion whether to further refine a triangular (or tetrahedral) element.

5.2 Results on the forward problem

The first step in solving the geoelectrical inverse problem was achieved by implementing the discrete forward operator by a finite element method. Figure 5 illustrates solutions generated by the finite element program for a constant conductivity coefficient σ. Various current patterns have been applied to 14 pike shaped electrodes placed at the boundary. The spatial frequency of the current patterns increases from the upper left to the lower right figure.

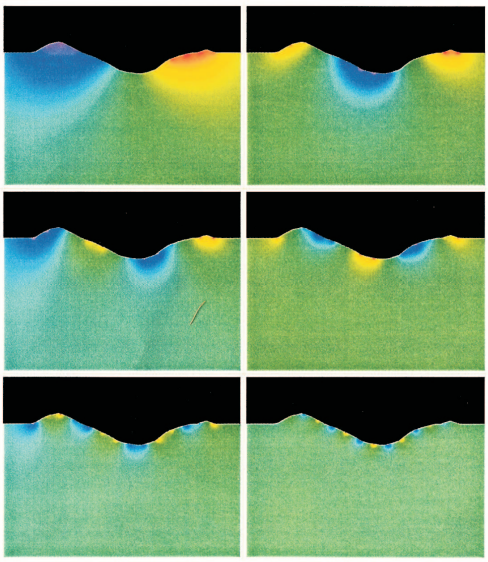

Figure 5: Potential distributions generated by various current patterns.

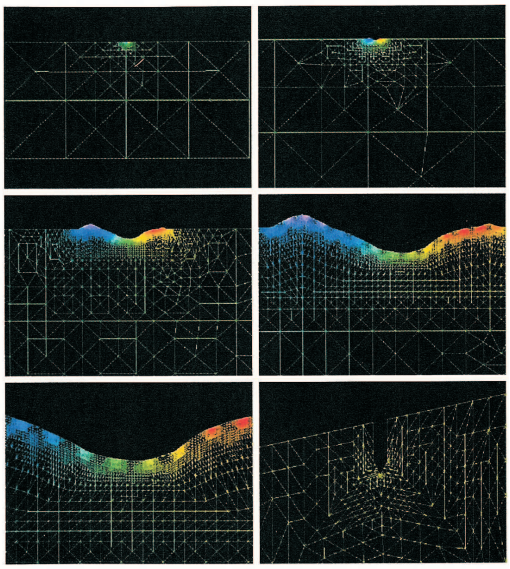

Figure 6: Adaptively refined FEM mesh

5.3 Adaptively refined meshes

To solve the geoelectrical forward problem numerically, the rapidly changing behaviour of solutions near the electrodes needs to be considered. This behaviour is due to the electrode geometry and the boundary conditions introduced by the electrode model.

In contrast to the rapid variation of the potential near electrodes, at large distance from current sources the solution changes very slowly. We decided to model these various kinds of behaviour by adaptively refined meshes of triangles or tetrahedrons. The refinement process starts with a coarse triangulation with large triangles at large distances from electrodes but the adaptive refinement procedure introduces many small triangles near the electrodes. The process of refining finite element meshes is well known but nevertheless tedious to implement. For technical details of the mesh refinement cf. [35, 37].

Figure 6 shows a mesh in various scales. The data for this example is the same used for that one shown in Figure 5.

To solve the problem numerically, some simplifications must be performed otherwise the implementation became too expensive and the algorithms were much too slow. The spaces $X := L^2(\Omega)$ and $Y := \mathbb{R}^l$ have been chosen for implementing the nonlinear minimization. Using the space $L^2(\Omega)$ as parameter space violates the assumptions of the convergence analysis of Chapter 4 but nevertheless, leads to satisfactory results and convergence rates. The discretization is achieved by an adaptively refined triangulation Ω_h, which remains fixed throughout the reconstruction. The space of parameter functions was chosen to be $\mathcal{P}_h \subset L^2(\Omega)$ with respect to the triangulation Ω_h to solve approximately

the inverse problem the minimization of

$$T_a^\delta(\sigma) := \|A(\sigma) - y^\delta\|_{l^2}^2 + \alpha\|\sigma - \sigma^+\|_{L^2(\Omega)}^2, \tag{46}$$

must be performed. To achieve this minimization, the Gauß-Newton method was chosen to be implemented. This requires that at each iteration we solve numerically the linear problem

$$\begin{aligned} Qd_{k+1} &= b, \quad \text{where} && (47)\\ Q &= \mathcal{DA}(\sigma_k)^+\mathcal{DA}(\sigma_k) + \alpha I \quad \text{and} && (48)\\ b &= \mathcal{DA}(\sigma_k)^+\left(y^\delta - A(\sigma_k)\right) + \alpha(\sigma^+ - \sigma_k) && (49) \end{aligned}$$

which leads to the update $\sigma_{k+1} = \sigma_k + d_{k+1}$. This is repeated until the residuum $\|A(\sigma_{k+1}) - y^\delta\|_{l^2}$ becomes sufficiently small. Solving the linear problem is achieved using the conjugate gradient method. The most expensive step there is the evaluation of the expression Qd_k, which requires us to solve the boundary value problem twice for each component A_j. The system matrix M_{σ_k} $(= M_\sigma)$ depends only on σ_k which is fixed when solving the linear problem. Using an LU sparse matrix solver leads to an efficient implementation since, for solving the $2 \times (l-1) \times (no.\ of\ CG\ iterations)$ boundary value problems (with various right hand sides), a single LU decomposition can be used. LU decomposition and forward-backward substitution is performed using the Harwell-MA28 sparse matrix solver [14].

5.4 Optimal choice of regularization parameter

The following sequence of reconstructions with increasing regularization parameter α demonstrates how the damping of data errors within the inversion process depends on α. The model shown in Figure 7 was used to calculate the data. An error of 1% was added and the resulting perturbed data was used for each reconstruction. The sequence starts with small α. Figure 10 is related to this sequence and shows the corresponding reconstruction errors.

This demonstrates that the choice of α is crucial for the inversion of real data. A systematic study of parameter choice rules will not be given here and for a thorough discussion of this topic we again recommend [18].

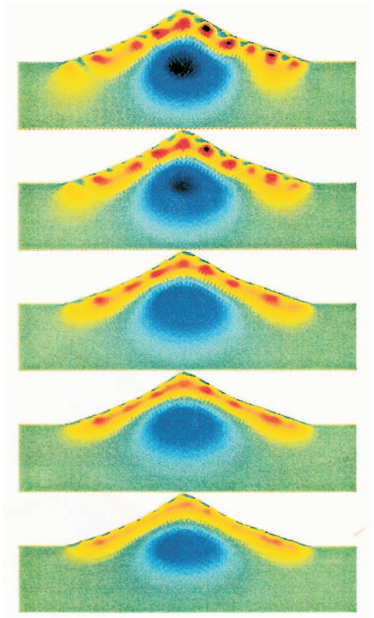

Figure 7: Reconstructions for various α and a fixed error level $\delta = 1.0\%$.

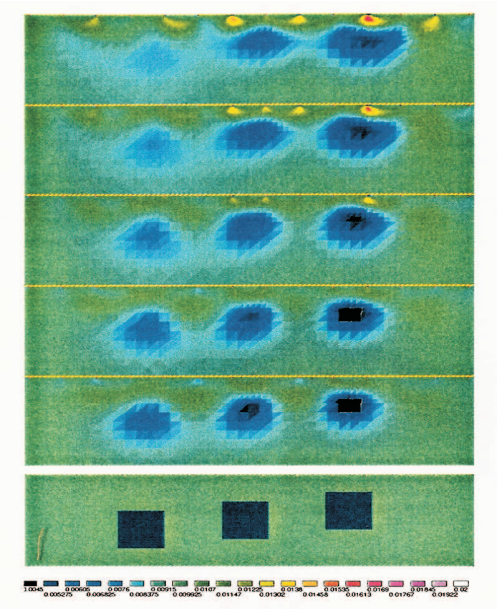

Figure 8: Reconstructions for various δ and $\alpha \sim \delta$; bottom: prescribed model function

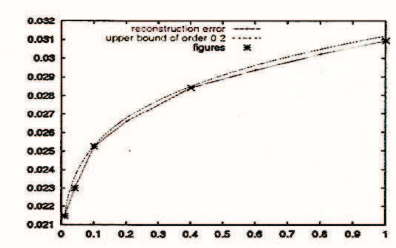

Figure 9: L^2-reconstruction-error plotted against different error levels δ.

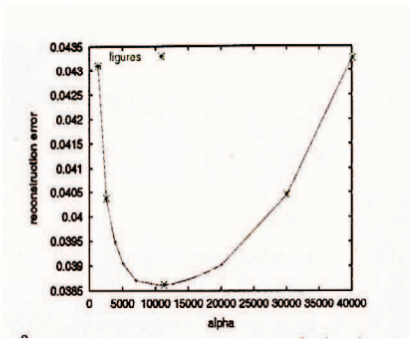

Figure 10: L^2-reconstruction-error plotted against regularization parameter α

5.5 Convergence rates

The aim of this section is to study convergence rates obtained by the implemented reconstruction algorithm and to compare them with the convergence rates stated in the previous section. This task is achieved for a simple example. It includes very low contrasts, i.e., the parameter varies slowly within the interval $[0.01, 0.012]$ in order to approximate a smooth function which provides a small ϑ value. Unfortunately, the x^*-minimum-norm solution is not available and hence the reconstruction-error can only be calculated with respect to the

prescribed model function. The measured convergence rate is of order 0.4 which is very close to the theoretical expected 0.5. Figure 9 shows the reconstruction errors for different levels of data error δ. This seems very satisfactory taking into account that the reconstruction algorithm violates the assumptions which were sufficient for establishing the convergence analysis (the minimization of the Tikhonov functional was implemented with respect to the L^2-norm and not with respect to the theoretically required H^2-norm). Note that this example includes only very low contrasts and therefore more accurate data is needed to recover the structure of the conductivity coefficient.

The calculations for this example was achieved without the use of weight functions and by applying the theoretically suggested parameter choice strategy $\alpha = K\delta$, where K was determined to be optimal for the greatest error level of consideration ($\delta = 1\%$). At the boundary 14 pike shape electrodes were placed equidistantly for simulating the data.

We finally conclude with a 3D reconstruction, which was obtained from simulated data with an 1% error level. We want to emphasise that the simulated data were obtained with a different, finer grid compared with that used in the reconstruction algorithm.

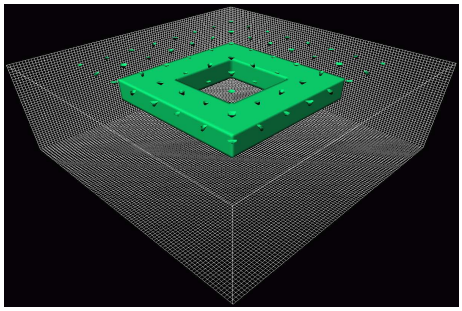

Figure 11: 3D-model of an underground structure, the layout of the electrodes on the surface is marked.

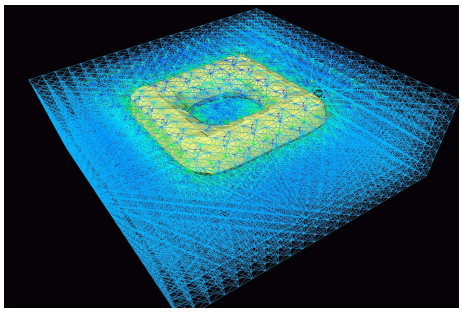

Figure 12: Reconstructions for $\delta = 1\%$ and $\alpha \sim \delta$.

References

[1] Alessandrini G, 'Singular solutions of elliptic equations and the determination of conductivity by boundary measurements', *J. Diff. Eq.* Vol **84**, 252-273 (1990).

[2] Barber D C and Brown B H, 'Recent developments in applied potential tomography - APT', *In S. L. Bacharach and M. Nijhoff, editors, Information Processing in Medical Imaging*, 106-121 (1986)

[3] Borcea, L, Berryman J and Papanicolaou, 'High contrast impedance imaging' *Inverse Problems* Vol **12**, 835-858 (1996).

[4] Brown R M, Uhlmann G A, 'Uniqueness in the inverse conductivity problem for nonsmooth conductivities in two dimensions', *Comm. in Part. Diff. Equ.* Vol **22(5** & **6)**, 1009-1027, (1997).

[5] Brühl M,'Explicit characterization of inclusions in electrical impedance tomography', *SIAM J Math Anal* Vol **2**, 1327-1341 (2001).

[6] Brühl M and Hanke M , 'Numerical implementation of two non-iterative methods for locating inclusions by impedance tomography', *Inverse Problems* Vol **16**, 1029-1042 (2000).

[7] Brühl M, Hanke M and Vogelius M, 'A direct impedance tomography algorithm for locating small inhomogeneities' *preprint* (2001).

[8] Calderon A P, 'On an inverse boundary value problem', *In Seminar on Numerical Analysis and Its Applications to Continuum Physics, Rio de Janeiro, Sociedade Brasileira de Matematica*, 67-73 (1980).

[9] Cedio-Fengya, D, Moskow S and Vogelius M, Identification of conductivity imperfections by boundary measurements. Continuous dependence and computational reconstruction. *Inverse Problems* Vol **14**, 553-595 (1998).

[10] Ciulli S, Pidcock M K and Stroian A, 'Image reconstruction in electrical impedance tomography using an integral equation of the Lippmann-Schwinger type', *Physics Letters A* 271, 377-384 (2000).

[11] Dey A and Morrison H F,'Resistivity modelling for arbitrarily shaped two-dimensional structures', *Geophysical Prospecting* Vol **27** 106-136, (1979).

[12] Dicken V, 'A new approach towards simultaneous activity and attenuation aeconstruction in emission tomography', *Inverse Problems* Vol **15(8)** 931-960, (1999).

[13] Druskin V, 'On the uniqueness of inverse problems from incomplete boundary data', *SIAM J. Appl. Math.* Vol **58(5)** 1591-1603, (1998).

[14] Duff I S, 'Ma28 - a set of Fortran subroutines for sparse unsymmetric linear equations', Tech. Report AERE-R 8730, Harwell, (1980).

[15] Isakov V, 'On uniqueness of recovery of a discontinuous conductivity coefficient', *Comm. Pure Appl. Math.* Vol **41** 865 - 877, (1988).

[16] Hofmann B, 'Approximation of the inverse electrical impedance tomography problem by an inverse transmission problem', *Inverse Problems* Vol **14** 1171-1187,(1998).

[17] Ellis R G and Oldenburg D W, 'Applied geophysical inversion', *Geophys J. Int.* Vol **116** 5-11, (1994).

[18] Engl H, Hanke M, Neubauer A, 'Regularization of Inverse Problems', *Kluwer Acad. Publ., Dordrecht*, (1996).

[19] Engl H W, Kunisch K and Neubauer A, 'Convergence rates for Tikhonov regularization of nonlinear ill-posed problems', *Inverse Problems* Vol **5** 523-540, (1989).

[20] Vauhkonen M, Kaipio J, Somersalo E and Kajaloinen P, 'Electrical impedance Tomography with basis constraints', *Inverse Problems* Vol 13, 523-530 (1997).

[21] Friedel S, Flechsig Ch, Klimmek R and Proeck I, 'Geoelektrische Untersuchungen am Dekadenvulkan Merapi auf Java(Indonesien)', *Proceeding:57. Jahrestagung der Deutschen Geophysikalischen Gesellschaft* Potsdam (1997).

[22] Hanke M, 'A regularizing Levenberg Marquart scheme, with applications to groundwater filtration problems', *Inverse Problems* Vol **13** 79-95, (1997).

[23] Hettlich F and Rundell W, 'The deternination of a discontinuity from a single boundary measurement', *Inverse Problems*, Vol 14, 67-82, (1998).

[24] Isaacson D,'Distinguishability of conductivities by electric current computed tomography', *IEEE Trans. Med. Imag.* Vol **MI-5** 91-95, (1986).

[25] Janssen R, 'Elliptic problems on unbounded domains', *SIAM J. MATH. ANAL.* Vol **17/6**, (1986).

[26] Kohn R and Vogelius M, 'Determining conductivity by boundary measurements',*Comm. Pure Appl. Math.*, Vol **37** 289-298, (1984).

[27] Kohn R and Vogelius M, 'Determining conductivity by boundary measurements II. Interior results', *Comm. Pure Appl. Math*, Vol **8** 643-667, (1985).

[28] Li D and Oldenburg W, 'Inversion of 3-D DC resistivity data using an approximate inverse mapping', *Geophys. J. Int.* Vol **116** 527-537, (1994).

[29] Loke M H and Barker R D, 'Rapid least-squares inversion of apparent resistivity pseudosections by a quasi-newton method', *Geophysical Prospecting* Vol **44** 131-152, (1996).

[30] Louis A K, 'Inverse und schlecht gestellte Probleme', *Teubner, Stuttgart*, (1989).

[31] Lukaschewitsch M, 'Inversion of Geoelectric Boundary Data, a Nonlinear Ill-Posed Problem', *PhD thesis, Universität Potsdam*, (1999).

[32] Nachman A I, Sylvester J and Uhlmann G, 'An n-dimensional Borg-Levinson theorem.', *Comm. Math. Phys.*, Vol **115** 593-605, (1988).

[33] Nachman A, 'Global uniqueness for a two dimensional inverse boundary value problem', *Ann. Math.*, Vol 142, 71-96, (1995).

[34] Pidcock M, Ciulli S and Ispas S, 'Singularities of mixed boundary value problems in electrical impedance tomography ', *Physiol. Meas.*, Vol **16** A213-A218, (1995).

[35] P. Leinen, Deuflhard P and Yserentant H, 'Concepts of an adaptive hierarchical finite element code', *Impact of Computing in Science and Engineering*, Vol **1** 3-35, (1989).

[36] Paulson K, Lionheart W and Pidcock M, 'POMPUS: an optimized reconstruction algorithm' *Inverse Problems* Vol 11, 425-437, 1995.

[37] B. Erdmann, R. Beck, R. Roitzsch. Kaskade 3.0, Tech. Rep. ZIB Berlin, Takustr. 7, D-14195 Berlin, 1995.

[38] Siltanen S, Mueller J and Isaacson D, 'An implementation of the reconstruction algorithm of A Nachman for the 2D inverse conductivity problem' *Inverse Problems* Vol 16, 681-699 (2000).

[39] Spiegelberg H, Danckwardt E, Flechsig Ch, Jacobs F and Storz W, 'Gleichstromgeoelektrik zur Erkundung der Leitfähigkeitsverteilung der Erdkruste - Ergebnisse des Dipol-Dipol-Experiments an der KTB', *Tagungsband: VI: Arbeitsseminar "Hochauflsende Geoelektrik, Bucha Universität Leipzig, Institut für Geophysik und Geologie*, (1997).

[40] Sylvester J and Uhlmann G, 'A global uniqueness theorem for an inverse boundary value problem', *Ann. of Math.*, Vol **125** 153-169, (1987).

[41] Sylvester J and Uhlmann G, 'Inverse boundary value problems at the boundary - Continuous dependence', *Comm. Pure Appl. Math.*, Vol **41** 197-221, (1988).

[42] Triebel H, 'Theory of Function Spaces', *Leipzig, Geest und Portig, Basel, Birkhäuser*, (1983).

[43] Worzyk P, 'Geoelektrische Untersuchungen im Bereich der Hagenower Rinne', *Tagungsband: VII. Arbeitsseminar "Hochauflösende Geoelektrik, Bucha. Universitt Leipzig, Institut für Geophysik und Geologie*, (1989).

Berichte aus der Technomathematik ISSN 1435-7968

http://www.math.uni-bremen.de/zetem/berichte.html

— Vertrieb durch den Autor —

Reports **Stand: 11. Oktober 2002**

98–01. Peter Benner, Heike Faßbender:
An Implicitly Restarted Symplectic Lanczos Method for the Symplectic Eigenvalue Problem, Juli 1998.

98–02. Heike Faßbender:
Sliding Window Schemes for Discrete Least-Squares Approximation by Trigonometric Polynomials, Juli 1998.

98–03. Peter Benner, Maribel Castillo, Enrique S. Quintana-Ortí:
Parallel Partial Stabilizing Algorithms for Large Linear Control Systems, Juli 1998.

98–04. Peter Benner:
Computational Methods for Linear–Quadratic Optimization, August 1998.

98–05. Peter Benner, Ralph Byers, Enrique S. Quintana-Ortí, Gregorio Quintana-Ortí:
Solving Algebraic Riccati Equations on Parallel Computers Using Newton's Method with Exact Line Search, August 1998.

98–06. Lars Grüne, Fabian Wirth:
On the rate of convergence of infinite horizon discounted optimal value functions, November 1998.

98–07. Peter Benner, Volker Mehrmann, Hongguo Xu:
A Note on the Numerical Solution of Complex Hamiltonian and Skew-Hamiltonian Eigenvalue Problems, November 1998.

98–08. Eberhard Bänsch, Burkhard Höhn:
Numerical simulation of a silicon floating zone with a free capillary surface, Dezember 1998.

99–01. Heike Faßbender:
The Parameterized SR Algorithm for Symplectic (Butterfly) Matrices, Februar 1999.

99–02. Heike Faßbender:
Error Analysis of the symplectic Lanczos Method for the symplectic Eigenvalue Problem, März 1999.

99–03. Eberhard Bänsch, Alfred Schmidt:
Simulation of dendritic crystal growth with thermal convection, März 1999.

99–04. Eberhard Bänsch:
Finite element discretization of the Navier-Stokes equations with a free capillary surface, März 1999.

99–05. Peter Benner:
Mathematik in der Berufspraxis, Juli 1999.

99–06. Andrew D.B. Paice, Fabian R. Wirth:
Robustness of nonlinear systems and their domains of attraction, August 1999.

99–07. Peter Benner, Enrique S. Quintana-Ortí, Gregorio Quintana-Ortí:
Balanced Truncation Model Reduction of Large-Scale Dense Systems on Parallel Computers, September 1999.

99–08. Ronald Stöver:
Collocation methods for solving linear differential-algebraic boundary value problems, September 1999.

99–09. Huseyin Akcay:
Modelling with Orthonormal Basis Functions, September 1999.

99–10. Heike Faßbender, D. Steven Mackey, Niloufer Mackey:
Hamilton and Jacobi come full circle: Jacobi algorithms for structured Hamiltonian eigenproblems, Oktober 1999.

99–11. Peter Benner, Vincente Hernández, Antonio Pastor:
On the Kleinman Iteration for Nonstabilizable System, Oktober 1999.

99–12. Peter Benner, Heike Faßbender:
A Hybrid Method for the Numerical Solution of Discrete-Time Algebraic Riccati Equations, November 1999.

99–13. Peter Benner, Enrique S. Quintana-Ortí, Gregorio Quintana-Ortí:
Numerical Solution of Schur Stable Linear Matrix Equations on Multicomputers, November 1999.

99–14. Eberhard Bänsch, Karol Mikula:
Adaptivity in 3D Image Processing, Dezember 1999.

00–01. Peter Benner, Volker Mehrmann, Hongguo Xu:
Perturbation Analysis for the Eigenvalue Problem of a Formal Product of Matrices, Januar 2000.

00–02. Ziping Huang:
Finite Element Method for Mixed Problems with Penalty, Januar 2000.

00–03. Gianfrancesco Martinico:
Recursive mesh refinement in 3D, Februar 2000.

00–04. Eberhard Bänsch, Christoph Egbers, Oliver Meincke, Nicoleta Scurtu:
Taylor-Couette System with Asymmetric Boundary Conditions, Februar 2000.

00–05. Peter Benner:
Symplectic Balancing of Hamiltonian Matrices, Februar 2000.

00–06. Fabio Camilli, Lars Grüne, Fabian Wirth:
A regularization of Zubov's equation for robust domains of attraction, März 2000.

00–07. Michael Wolff, Eberhard Bänsch, Michael Böhm, Dominic Davis:
Modellierung der Abkühlung von Stahlbrammen, März 2000.

00–08. Stephan Dahlke, Peter Maaß, Gerd Teschke:
Interpolating Scaling Functions with Duals, April 2000.

00–09. Jochen Behrens, Fabian Wirth:
A globalization procedure for locally stabilizing controllers, Mai 2000.

00–10. Peter Maaß, Gerd Teschke, Werner Willmann, Günter Wollmann:
Detection and Classification of Material Attributes – A Practical Application of Wavelet Analysis, Mai 2000.

00–11. Stefan Boschert, Alfred Schmidt, Kunibert G. Siebert, Eberhard Bänsch, Klaus-Werner Benz, Gerhard Dziuk, Thomas Kaiser:
Simulation of Industrial Crystal Growth by the Vertical Bridgman Method, Mai 2000.

00–12. Volker Lehmann, Gerd Teschke:
Wavelet Based Methods for Improved Wind Profiler Signal Processing, Mai 2000.

00–13. Stephan Dahlke, Peter Maass:
A Note on Interpolating Scaling Functions, August 2000.

00–14. Ronny Ramlau, Rolf Clackdoyle, Frédéric Noo, Girish Bal:
Accurate Attenuation Correction in SPECT Imaging using Optimization of Bilinear Functions and Assuming an Unknown Spatially-Varying Attenuation Distribution, September 2000.

00–15. Peter Kunkel, Ronald Stöver:
Symmetric collocation methods for linear differential-algebraic boundary value problems, September 2000.

00–16. Fabian Wirth:
The generalized spectral radius and extremal norms, Oktober 2000.

00–17. Frank Stenger, Ahmad Reza Naghsh-Nilchi, Jenny Niebsch, Ronny Ramlau:
A unified approach to the approximate solution of PDE, November 2000.

00–18. Peter Benner, Enrique S. Quintana-Ortí, Gregorio Quintana-Ortí:
Parallel algorithms for model reduction of discrete–time systems, Dezember 2000.

00–19. Ronny Ramlau:
A steepest descent algorithm for the global minimization of Tikhonov–Phillips functional, Dezember 2000.

01–01. Efficient methods in hyperthermia treatment planning:
Torsten Köhler, Peter Maass, Peter Wust, Martin Seebass, Januar 2001.

01–02. Parallel Algorithms for LQ Optimal Control of Discrete-Time Periodic Linear Systems:
Peter Benner, Ralph Byers, Rafael Mayo, Enrique S. Quintana-Ortí, Vicente Hernández, Februar 2001.

01–03. Peter Benner, Enrique S. Quintana-Ortí, Gregorio Quintana-Ortí:
Efficient Numerical Algorithms for Balanced Stochastic Truncation, März 2001.

01–04. Peter Benner, Maribel Castillo, Enrique S. Quintana-Ortí:
Partial Stabilization of Large-Scale Discrete-Time Linear Control Systems, März 2001.

01–05. Stephan Dahlke:
Besov Regularity for Edge Singularities in Polyhedral Domains, Mai 2001.

01–06. Fabian Wirth:
A linearization principle for robustness with respect to time-varying perturbations, Mai 2001.

01–07. Stephan Dahlke, Wolfgang Dahmen, Karsten Urban:
Adaptive Wavelet Methods for Saddle Point Problems - Optimal Convergence Rates, Juli 2001.

01–08. Ronny Ramlau:
Morozov's Discrepancy Principle for Tikhonov regularization of nonlinear operators, Juli 2001.

01–09. Michael Wolff:
Einführung des Drucks für die instationären Stokes–Gleichungen mittels der Methode von Kaplan, Juli 2001.

01–10. Stephan Dahlke, Peter Maaß, Gerd Teschke:
Reconstruction of Reflectivity Desities by Wavelet Transforms, August 2001.

01–11. Stephan Dahlke:
Besov Regularity for the Neumann Problem, August 2001.

01–12. Bernard Haasdonk, Mario Ohlberger, Martin Rumpf, Alfred Schmidt, Kunibert G. Siebert:
h–p–Multiresolution Visualization of Adaptive Finite Element Simulations, Oktober 2001.

01–13. Stephan Dahlke, Gabriele Steidl, Gerd Teschke:
Coorbit Spaces and Banach Frames on Homogeneous Spaces with Applications to Analyzing Functions on Spheres, August 2001.

02–01. Michael Wolff, Michael Böhm:
Zur Modellierung der Thermoelasto-Plastizität mit Phasenumwandlungen bei Stählen sowie der Umwandlungsplastizität, Februar 2002.

02–02. Stephan Dahlke, Peter Maaß:
An Outline of Adaptive Wavelet Galerkin Methods for Tikhonov Regularization of Inverse Parabolic Problems, April 2002.

02–03. Alfred Schmidt:
A Multi-Mesh Finite Element Method for Phase Field Simulations, April 2002.

02–04. Sergey N. Dachkovski, Michael Böhm:
A Note on Finite Thermoplasticity with Phase Changes, Juli 2002.

02–05. Michael Wolff, Michael Böhm:
Phasenumwandlungen und Umwandlungsplastizität bei Stählen im Konzept der Thermoelasto-Plastizität, Juli 2002.

02–06. Gerd Teschke:
Construction of Generalized Uncertainty Principles and Wavelets in Anisotropic Sobolev Spaces, August 2002.

02–07. Ronny Ramlau:
TIGRA – an iterative algorithm for regularizing nonlinear ill–posed problems, August 2002.

02–08. Michael Lukaschewitsch, Peter Maaß, Michael Pidcock:
Tikhonov regularization for Electrical Impedance Tomography on unbounded domains, Oktober 2002.